ELSEVIER

Composites Science and Technology 60 (2000) 255–261

COMPOSITES SCIENCE AND TECHNOLOGY

A predictive creep model for un-stitched and stitched woven composites

Feiyi Pang [a], Chun Hui Wang [b,*]

[a] *Centre for Composite Materials, University of Delaware, Newark, DE 19716-3144, USA*
[b] *Aeronautical and Maritime Research Laboratory, 506 Lorimer Street, Fishermans Bend, VIC 3207, Australia*

Received 11 January 1999; received in revised form 14 July 1999; accepted 9 August 1999

Abstract

Previous studies have shown that woven carbon composites exhibit considerable creep even at ambient temperature, and that through-thickness stitching can significantly reduce the creep rate. This article presents a mechanistic model for quantifying the time-dependent creep of woven carbon fibre composites, assuming that the carbon fibres remain elastic and the matrix is linear visco-elastic. It is shown that the predictions of the model are in close agreement with experimental results for both unstitched and stitched woven carbon composites.

Keywords: B. Creep; Stitching; Woven composites; Visco-elasticity

1. Introduction

Creep can occur in fibre/polymer composites, even at ambient temperature, because of the visco-elastic–plastic deformation of the resin matrix, although the fibres do not normally creep. The creep behaviour of composites is related mainly to the geometry and the material properties of constituents. Previous studies [1–4] have show that fibre-reinforced epoxy composite laminates exhibited some creep even at ambient temperature. Various models of creep deformation of composite materials have been developed to describe such creep behaviour. McLean [5] published a number of creep models and compared them with experimental data. The implications of the rule of mixtures were discussed when (a) both the matrix and the reinforcing phase are subject to creep deformation and (b) the reinforcement extends elastically in a creeping matrix, with particular emphasis on the establishment of steady-state creep and the representation of creep data for composites. Dillard et al. [6] considered creep and creep rupture of laminated carbon/epoxy composites. Laminated fibre composites such as carbon/epoxy are generally designed on the basis of elastic considerations, as cross-ply laminates are often considered to be immune from creep. However, since the epoxy matrix in a fibre-reinforced composite behaves in a visco-elastic manner, the resulting carbon/epoxy composite material may exhibit creep and delayed failures, depending on the architecture of the composite.

Raghavan [7] proposed an activation theory for the creep of the matrix resin and a carbon-fibre-reinforced polymer composite. Chen et al. [8] and Haddad and Tanary [9] used Eshelby's inclusion principle and the Mori and Tannaka micromechanics formulation to predict composite creep. Using the Laplace transform method, Dominguez et al. [10] analysed the creep response of linear visco-elastic carbon/epoxy composites. The creep and relaxation responses of a composite made of angle-ply lay-ups of a medium toughness carbon/epoxy system were correlated by using Maxwell/Kelvin-type models. Calculations of normalized creep compliance responses from short relaxation tests were compared to normal creep compliance values. Rand [11] developed a non-linear visco-elastic creep model to predict the strains at a stress level approaching the yield stress of the polymer. Specific results were presented for a 20 μm blown film extruded from a linear low-density polyethylene resin with exceptional low-temperature deformation capabilities. Ericksen [12] tested Kevlar-49/epoxy composites and compared the theoretical and experimental results using Garmong's analysis. It was found

* Corresponding author. Tel.: +61-3-9626-7121/25; fax: +61-3-9626-7089.
E-mail address: chun-hui.wang@dsto.defence.gov.au (C.H. Wang).

0266-3538/00/$ - see front matter
PII: S0266-3538(99)00117-7

that the accuracy of model simulations of the creep behaviour of a composite was dependent on the applicability of the assumed constitutive equation of each constituent. Goto [13] investigated the slipping effect at fibre/matrix interfaces of continuous and short-fibre composites.

Unidirectional or bi-directional carbon composite materials are often regarded as being immune from creep at ambient temperature, primarily because the fibres would remain elastic even at stress levels close to their failure strength [14]. However, woven composites have been found to exhibit considerable creep even at ambient temperature [14]. This sharp contrast between the creep behaviour of cross-ply laminates with 0/90 lay-ups and woven composites is rather unexpected, raising a question regarding the possible underlying mechanisms and whether it is possible to quantify such a phenomenon.

In woven-carbon-fibre composites where the fibres should remain elastic, there are two potential mechanisms by which woven composites can creep: (i) changes in the waviness of the fibres induced by the creep of the matrix and (ii) slippage between fibres embedded in a creeping matrix. In the present work, it is postulated that the change in waviness is the primary cause of the observed creep at ambient temperature. At elevated temperatures, slippage between fibres may become a significant issue. The purpose of this article is to present a mechanistic model for describing the time-dependent undulation of the fibre weft and then establish a kinetic relationship to quantify the total creep of woven composites; slippage between fibres and the matrix is not addressed. Comparison will then be made with experimental results for both un-stitched and stitched composites.

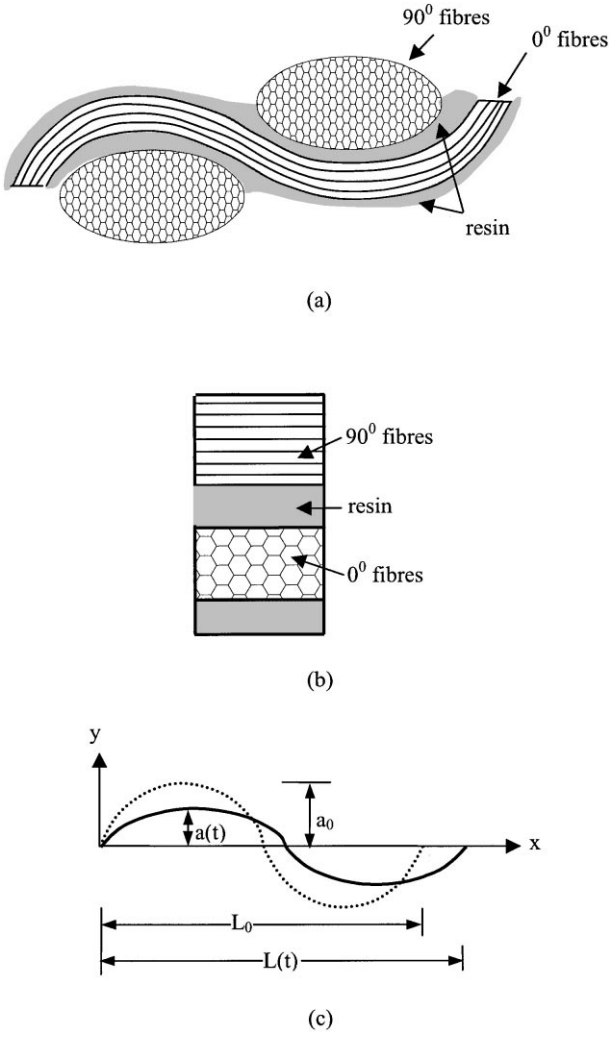

Fig. 1. A schematic illustration of weft and warp tows: (a) a section parallel to the specimen axis, (b) a section perpendicular to the specimen axis, and (c) geometry and notations for the waviness of a weft tow.

2. A model for the creep of woven composites

A two-dimensional idealisation of a unit cell of a typical woven composite is depicted in Fig. 1. Assume that the woven fibre undulation can be represented by a sinusoidal function,

$$y(x,t) = a(t)\sin\left(\frac{2\pi x}{L(t)}\right) \tag{1}$$

where a and L represent, respectively, the magnitude and wavelength of the fibre wave, and y denotes the height of the wave at position x and time t. Since the carbon fibres ought to remain elastic, no creep deformation will occur within the fibres. Therefore, the total length of the fibre should remain constant at any time, before and after subtraction of the initial elastic deformation. This implies that,

$$\int_0^{L_0}\sqrt{1+[y'(0,x)]^2}\,\mathrm{d}x = \int_0^{L(t)}\sqrt{1+[y'(t,x)]^2}\,\mathrm{d}x \tag{2}$$

Since $\| y'(t,x) \| << 1$ for most woven composites, the above equation can be well approximated as, noting Eq. (1),

$$\int_0^{L_0}\left\{1+\frac{1}{2}a_0^2\left(\frac{2\pi}{L_0}\right)^2\cos^2\left(\frac{2\pi x}{L_0}\right)\right\}\mathrm{d}x = \int_0^{L(t)}\left\{1+\frac{1}{2}a^2(t)\left(\frac{2\pi}{L(t)}\right)^2\cos^2\left(\frac{2\pi x}{L(t)}\right)\right\}\mathrm{d}x \tag{3}$$

where L_0 denotes the initial wavelength, and a_0 the initial magnitude. Therefore:

$$L_0 + \frac{a_0^2\pi^2}{L_0} = L(t) + \frac{a^2(t)\pi^2}{L(t)} \tag{4}$$

which leads to,

$$L(t) = \frac{1}{2}\left(L_0 + \frac{\pi^2}{L_0^2}a_0^2 - \sqrt{(L_0 + \frac{a_0^2\pi^2}{L_0^2})^2 - 4a^2(t)\pi^2}\right) \quad (5)$$

Now the longitudinal strain of the woven composite can be expressed as, according to definition:

$$\varepsilon_x^c(t) = \frac{L(t) - L_0}{L_0} \approx \frac{\pi^2\left(a_0^2 - a^2(t)\right)}{L_0^2} \quad (6)$$

By differentiating Eq. (6) the longitudinal creep rate of the woven composite can be readily obtained,

$$\dot{\varepsilon}_x^c(t) = -\frac{2\dot{a}(t)a(t)}{L_0^2}\pi^2 \quad (7)$$

It is now clear that the key to determining the longitudinal creep strain of woven composites is to quantify the evolution of the amplitude $a(t)$ with time, which is induced by the creep of the matrix in the direction perpendicular to the fibre direction.

Let us consider the creep deformation of the matrix in the lateral direction. A unit cell is shown in Fig. 1(c). Again, of the two phases, the fibres do not creep in the lateral direction, while the matrix (sum of the resin phase and the resin contained in the 0° fibre and 90° fibre phases) does creep. Adopting the linear visco-elasticity theory, the creep rate of the matrix phase in the y direction can be expressed as,

$$\dot{\varepsilon}_y^m = \sigma_y\left(\frac{1}{\eta_1} + \frac{1}{\eta_2}e^{-Rt/\eta_2}\right) \quad (8)$$

where σ_y denotes the interlaminar normal stress which will be determined later. The parameter R can be interpreted as a linear spring constant or the Young's modulus of the neat resin. The constants η_1 and η_2 are the coefficients of viscosity of the resin. For instance, in the present case the creep parameters for the resin at room temperature are $R = 180$ MPa, $\eta_1 = 500$ MPa h, and $\eta_2 = 100$ MPa h as measured from neat resin [15].

Since the transverse strain in the woven composite is likely to be relatively small, it would suffice to adopt the small-strain definition. Consequently the transverse strain in the woven composite is,

$$\varepsilon_y^c = \frac{a(t) - a_0}{a_0} \quad (9)$$

where:

$$a(t) = h_r(t) + h_f \quad (10)$$

with $h_r(t)$ and h_f denoting respectively the heights of the resin and the fibre phases. Since the fibre phase does not creep, i.e. h_f=const, Eq. (9) can be rewritten as:

$$\varepsilon_y^c = \frac{h_r(t) - h_{r0}}{a_0} \quad (11)$$

where h_{r0} denotes the initial height of the resin phase. The transverse strain pertaining to the resin phase is defined as, adopting the true strain definition to account for the relatively large visco-elastic deformation in the adhesive,

$$\varepsilon_y^r = \ln\frac{h_r(t)}{h_{r0}} \quad (12)$$

By differentiating Eqs. (11) and (12), the following kinetics equation can be established which characterises the rate of dimension change in the vertical direction induced by the creep deformation of the resin phase,

$$\dot{\varepsilon}_y^m h_r(t) = \dot{\varepsilon}_y^c a_0 \quad (13)$$

where $\dot{\varepsilon}_y^m$ denotes the creep rate of the resin in the lateral direction.

Combining Eqs. (13) and (8) yields the creep rate of the woven composite in the lateral direction,

$$\dot{\varepsilon}_y^c = \frac{h_r(t)}{a_0}\dot{\varepsilon}_y^m = \frac{h_r(t)}{a_0}\sigma_y\left(\frac{1}{\eta_1} + \frac{1}{\eta_2}e^{-Rt/\eta_2}\right) \quad (14)$$

where $h_r(t)$ can be determined from Eq. (11) that can be re-written as,

$$\frac{h_r(t)}{a_0} = \frac{h_{r0}}{a_0} + \varepsilon_y^c \quad (15)$$

Now combine Eqs. (14) and (15),

$$\dot{\varepsilon}_y^c = \left(\varepsilon_y^c + \frac{h_{r0}}{a_0}\right)\sigma_y\left(\frac{1}{\eta_1} + \frac{1}{\eta_2}e^{-Rt/\eta_2}\right) \quad (16)$$

For simplicity, let us assume that the interlaminar stress σ_y remains constant during creep. In this case, integration of Eq. (16) leads to,

$$\varepsilon_y^c(t) = \frac{h_{r0}}{a_0}\left\{\exp\left[\sigma_y\left(\frac{t}{\eta_1} - e^{-Rt/\eta_2}\right)\right] - 1\right\} \quad (17)$$

It is easy to see from Eq. (17) that ε_y^c asymptotes to a limiting value of $-\frac{h_{r0}}{a_0}$ as time $t \to \infty$, provided that σ_y is negative (see Section 3). This asymptotic limit represents the final state when all the resin phase has been driven away from between the fibre phases and into the gaps between weft and warp tows.

From Eq. (17), the transverse creep rate of the woven composite is:

$$\dot{\varepsilon}_y^c(t) = \frac{h_{r0}}{a_0}\sigma_y\left[\frac{1}{\eta_1} + \frac{1}{\eta_2}e^{-Rt/\eta_2}\right]e^{\sigma_y\left[\frac{t}{\eta_1} - \frac{1}{R}e^{-Rt/\eta_2}\right]} \quad (18)$$

According to Eq. (9), the rate of $a(t)$ is given by:

$$\dot{a}(t) = h_{r0}\sigma_y\left(\frac{1}{\eta_1} + \frac{1}{\eta_2}e^{-Rt/\eta 2}\right)e^{\sigma_y\left(\frac{t}{\eta_1} - \frac{1}{R}^{-Rt/\eta_2}\right)} \quad (19)$$

By integrating Eq. (19) the amplitude of the waviness $a(t)$ can be obtained:

$$\begin{aligned} a(t) &= \int_0^t a(t)\mathrm{d}t + a_0 \\ &= h_{r0}e^{\sigma_y\left(\frac{t}{\eta_1} - \frac{1}{R}e^{-Rt/\eta_2}\right)} - h_{r0}e^{-\sigma_y/R} + a_0 \\ &= a_0 + h_{r0}\left(e^{\sigma_y\left(\frac{t}{\eta_1} - \frac{1}{R}e^{-Rt/\eta 2}\right)} - e^{-\sigma_y/R}\right) \end{aligned} \quad (20)$$

The asymptotic value of $a(t)$ in the limiting case of $t \to \infty$ is, assuming $-\sigma_y/R << 1$,

$$\lim_{t\to\infty} a(t) = a_0 - h_{r0} \quad (21)$$

which corresponds, as discussed earlier, to the expected limiting case when the resin phase has been almost completely squeezed out and forced into the gaps between the weft and warp tows.

From Eq. (6) the longitudinal creep strain can now be expressed as,

$$\varepsilon_x^c(t) = \frac{\pi^2 a_0^2}{L_0^2}\left(1 - \left(\frac{a}{a_0}\right)^2\right) = \frac{\pi^2 a_0^2}{L_0^2}\left(1 - \left(1 + \frac{h_{r0}}{a_0}\left(e^{\sigma_y\left(\frac{t}{\eta_1} - \frac{1}{R}e^{-Rt/\eta 2}\right)} - e^{-\sigma_y/R}\right)\right)^2\right) \quad (22)$$

with the following limiting value corresponding to $t \to \infty$,

$$\varepsilon_x^c(\infty) = \frac{\pi^2 a_0^2}{L_0^2}\left(1 - \left(\frac{a}{a_0}\right)^2\right) = \frac{\pi^2 a_0^2}{L_0^2}\left(1 - \left(1 + \frac{h_{r0}}{a_0}\left(e^{\sigma_y\left(\frac{t}{\eta_1} - \frac{1}{R}e^{-Rt/\eta 2}\right)} - e^{-\sigma_y/R}\right)\right)^2\right) \quad (23)$$

Eq. (22) furnishes an explicit formula for the longitudinal creep rate of a woven composite material. The only remaining unknown is the interlaminar stress σ_y that will be determined in the next section. Comparison with experimental results will be shown in Section 4.

3. Finite-element modelling of interlaminar stresses

It is clear from the previous section that the interlaminar stresses that exist between plies play an important role in the creep of the woven composites. This is consistent with the findings of previous studies [14,15], that, reducing the interlaminer stresses (e.g. by stitching) would significantly reduce creep. In the following a finite-element analysis is presented, which is used to determine the interlaminar stresses in unstitched and stitched composites.

The geometry of a two-dimensional unit cell is measured from the woven composite specimens being considered, and then simplified to give the unit cells shown in Fig. 2(a) and (b) for the un-stitched and the stitched woven composites. The geometry was simplified to reduce the complexity but without sacrificing too much the accuracy of the stress analysis. The thickness of each layer of the unit cell is calculated by dividing the thickness of the woven composite by the number of plies. The unstitched and stitched models, shown as unit cells

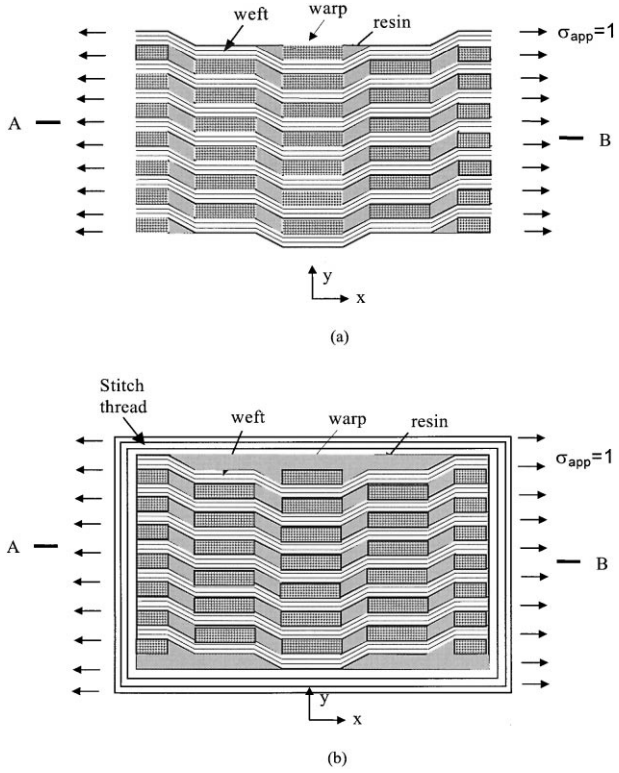

Fig. 2. Unit cells for (a) unstitched and (b) stitched woven composites (not to scale).

in Fig. 2(a) and (b), are constructed using two-dimensional, plane strain elements. The finite element analysis was conducted using a general purpose finite element code LUSAS.

To simplify the modelling of stitched and unstitched composites, it is imperative to make a minimum sacrifice in the representation of the finite element results. (1) The impregnated fibre tows (warp and weft yarns) are modelled with constant rectangular cross-sections (rather than elliptical sections). (2) The fibre volume fraction of the impregnated tows ($V_{\text{f.i.t.}}$) is assumed to be constant and the fibre volume fractions (V_{f}) of warp and weft tows are the same. (3) The unit cell behaves as an ideal composite so that voids and other such imperfections are negligible. (4) The properties used for the constituents in the unit cell (i.e. carbon fibre and epoxy resin) are taken to be those provided by the manufacturer for the actual materials used. The epoxy resin is assumed to be an isotropic material whilst the impregnated tows are assumed to be anisotropic. The material properties of the warp and weft tows are shown in Table 1. The elastic properties of the resin are $E = 3.2$ GPa, and Poisson's ratio is 0.35. The impregnated warp and weft tows were meshed using 8-node quadrilateral elements. The resin was modelled using triangular elements. The meshing used for the model consisted of 1470 nodes and 840 elements. A unit stress is applied at both the right-hand edge and the left-hand edge of the unit cell, as shown in Fig. 2. The main objective of the finite element analysis is to evaluate the interlaminar normal and shear stresses. In terms of the notations shown in Fig. 1, the dimensions for the unit cell correspond to: $a_0 = 0.1$ mm, $L_0 = 5.7$ mm and $h_{r0} = 0.01$ mm.

The distributions of the resulting shear stress τ_{xy} and normal stress σ_y along interface AB are shown in Fig. 3(a) and (b). These two stresses are believed to control the visco-elastic–plastic deformation and cracking of the matrix. Any creep in the matrix would lead to fibre straightening under the action of a tensile load. As can be seen in Fig. 3(a) and (b), both the shear and the normal stresses have been significantly reduced as a result of stitching. In particular, there is almost a two-fold reduction in the maximum values of the shear stress and the normal stress. The amount of reduction in these stresses is approximately equal to the increase in the stress required to cause the same amount of creep after stitching at a given time [14]. In other words, the enhanced creep resistance of stitched composites can be directly attributed to the reductions in the shear and normal stresses. This highlights that the main mechanism for the significant improvement in creep performance, by stitching, is the significant reduction in the interlaminar stresses.

To facilitate the following analysis, the average of the interlaminar normal stress over the region where the interlaminar stress is negative will be employed as a measure of the interlaminar stress that controls the lateral creep of the woven composite. From the finite element results, the following relation can be obtained,

$$\sigma_y = -A\sigma_{\text{app}} \tag{24}$$

where

$$A = \begin{cases} 0.26, & \text{unstitched composite} \\ 0.11, & \text{stitched composite} \end{cases} \tag{25}$$

Table 1
Material properties of the warp and weft non-undulated tows

Tow	E_1 (GPa)	E_2 (GPa)	ν_{12}
Weft	184.2	10.80	0.226
Warp	10.80	184.2	0.013

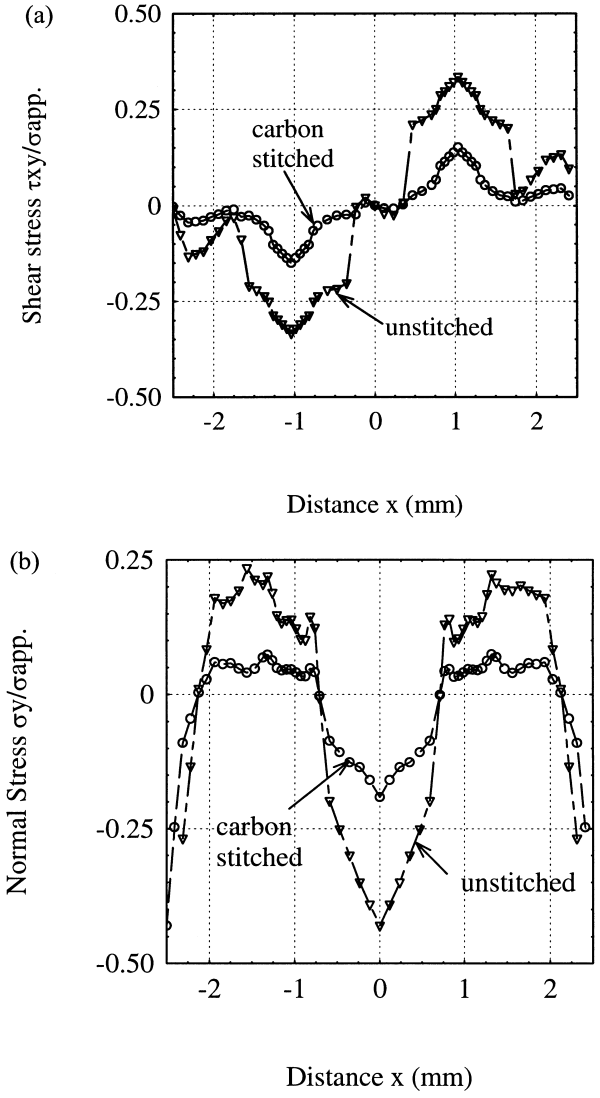

Fig. 3. Distribution of interlaminar stresses along AB: (a) shear stress and (b) normal stress.

These results provide a convenient means of determining the interlaminar normal stress in terms of the applied stress.

4. Comparison between predictions and experimental results

From previous analysis it is apparent that the longitudinal creep of a woven composite, stitched or unstitched, can be determined analytically, provided that the interlaminar normal stress in the resin is known. Due to the visco-elastic deformation associated with creep, the actual interlaminar stress in the resin would be coupled with the longitudinal creep, hence may gradually deviate from the initial condition. Nevertheless, it is not unreasonable to assume that, when the total lateral creep strain is small, the interlaminar stress remains approximately the same as if no creep is present. Therefore, we can approximate σ_y to be that obtained from the elastic solution presented in the previous section, Eq. (24).

To assess the accuracy of the present creep model, comparison will now be made with the experimental results. Such a comparison is shown in Fig. 4(a) and (b) for the unstitched composite tested under two different constant loads at room temperature. In these figures the solid lines represent the theoretical predictions, and the symbols represent the experimental results. It can be seen that the theoretical predictions are in reasonably good agreement with the experimental results at the two stress levels (70 and 90 MPa). The theoretical results for the carbon stitched composite are shown as curves in Fig. 5(a) and (b) for two stress levels (200 and 250 MPa), indicating a good correlation between the predictions and the experimental results.

Assuming that the fibres and matrix are always perfectly bonded, Eq. (22) predicts that as $t \to \infty$, the longitudinal strain asymptotically approaches an upper limit. However, the rate of approach is strongly dependent on whether the composite is stitched or unstitched. Stitched composites require higher stresses and longer times to reach the same creep strain at a given time. The theoretical analysis also allows us to study the amplitude of the waviness in stitched and unstitched composites. Tables 2 and 3 show the change of waviness after four days of testing. Prior to creep testing the unstitched and stitched composites have a waviness amplitude of 0.1 mm. After 4 days creep testing, the amplitudes of the carbon stitched sample, decreased to about 0.09 and 0.087 mm for applied stress levels of 200 and 250 MPa.

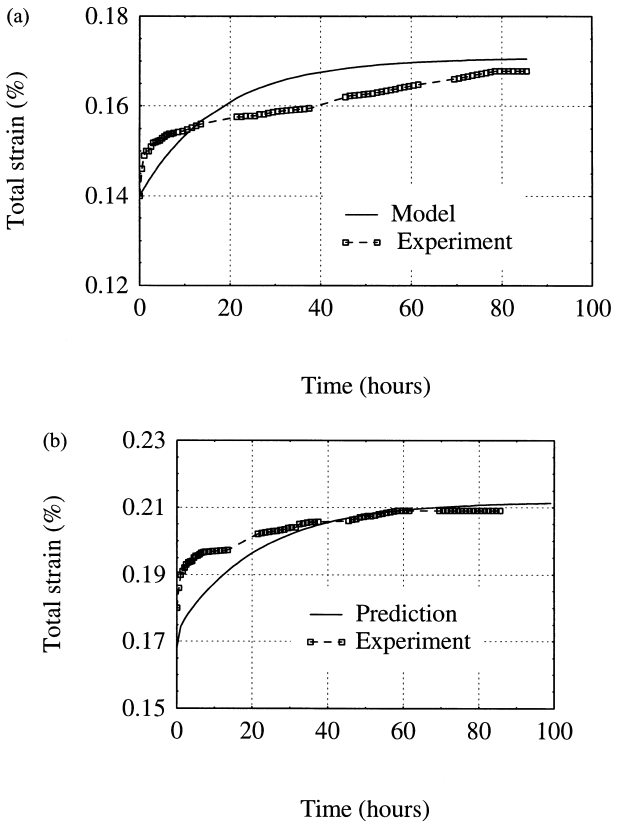

Fig. 4. Comparison between the theoretical predictions and the experimental data for the creep curves of the unstitched composite: (a) $\sigma_{app} = 70$ MPa and (b) $\sigma_{app} = 90$ MPa.

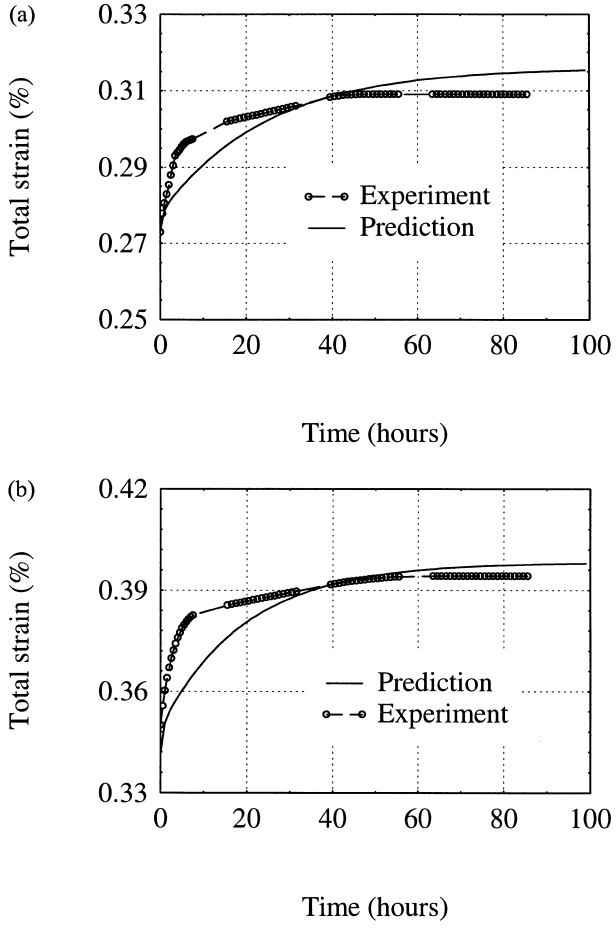

Fig. 5. Comparison between the theoretical predictions and the experimental data for the creep curves of the carbon stitched composite: (a) $\sigma_{app} = 200$ MPa and (b) $\sigma_{app} = 250$ MPa.

Table 2
Waviness of an unstitched composite

Stress (MPa)	Before creep testing (amplitude, mm)	After 4 days creep (amplitude, mm)	After 25 days creep (amplitude, mm)
70	0.1	0.088	0.085
90	0.1	0.086	0.085

Table 3
Waviness of 800 Tex carbon stitched composite

Stress (MPa)	Before creep testing (amplitude, mm)	After 4 days creep (amplitude, mm)	After 25 days creep (amplitude, mm)
200	0.1	0.09	0.085
250	0.1	0.087	0.085

For unstitched samples, the amplitudes decreased to 0.09 and 0.087 mm for stress levels of 70 and 90 MPa. The amplitude predicted by the present model is 0.085 mm for both the unstitched and the stitched composites. This means that the model correctly predicts fibre straightening, which is the main cause of the creep observed in woven composites. It should be mentioned, however, that the application of the present model is limited to woven composites with fibres at 0 and 90° to the load direction. It should also be noted that, in practice, delamination or interlaminar cracking may occur in an unstitched composite, thus leading to even higher creep strain.

5. Conclusions

A creep model is presented for woven carbon composites, which is shown to provide a good correlation with experimental results at room and elevated temperatures. It is found that the stitched and unstitched composites approached the same limit of creep strain, when the matrix and fibres are assumed to be perfectly bonded, without any void growth. However, stitched composites required higher stresses and longer times to induce the same level of creep strain than unstitched. The results showed that the present creep model can predict creep strains and creep rate for the woven structural composites.

The finite-element technique has been employed for analysing the deformation behaviour of periodic continuous woven fibre composites, stitched and unstitched. The results indicate that stitching significantly reduces the interlaminar stresses, hence confirming the beneficial effect of stitching in improving the creep resistance of woven composites.

References

[1] Lilholt H. Creep of fibrous composite materials. Comp Sci Technol 1985;22:277–94.
[2] Yen SC, Williamson FL. Accelerated characterisation of creep response of an off-axis composite material. Comp Sci Technol 1990;38:103–17.
[3] Zhu X, Li Z, Jin Y, Shaw WJD. Creep behaviour of a hybrid fibre (glass/carbon) — reinforced composite and its application. Comp Sci Technol 1994;50:431–9.
[4] Chung I, Sun CT, Chang IY. Modelling creep in thermoplastic composites. J Comp Mater 1993;27:1009–29.
[5] Mclean M. Creep deformation of metal-matrix composites. Comp Sci Technol 1985;23:37–52.
[6] Dillard DA, Morris DH, Brinson HF. Creep and creep rupture of laminated graphite/epoxy composites. Virginia Polytechnic Institute and State University Report No. VPI-E-81-3, Blacksburg, VA, 1981.
[7] Raghavan J, Meshii M. Activation theory for creep of matrix resin and carbon fibre-reinforced polymer composite. J Mater Sci 1994;29:5078–84.
[8] Chen CH, Chang YH, Cheng CH. Micromechanics and creep behaviour of fibre-reinforced Polyether-Ether-Ketone composites. J Comp Mater 1995;29:126.
[9] Haddad YM, Tanary S. On the Micromechanical characterisation of the creep response of a class of composite systems. J Pressure Vessel Technol 1989;111:117.
[10] Dominguez AR, Jordan WM. Predictive creep response of linear viscoelastic graphite/epoxy composites using the Laplace Transform Method. J Mater Eng Performance 1992;1:261.
[11] Rand JL. A nonlinear viscoelastic creep model. Tappi J 1995:178–182.
[12] Ericksen RH. Room temperature creep of Kevlar 49/Epoxy composites. Composites 1976;5:189–94.
[13] Goto S, Mclean M. Modeling interface effects during creep of metal matrix composite. Scripta Metall 1989;23:2073–8.
[14] Pang F, Wang CH, Bathgate RG. Creep response of woven-fibre composites and the effect of stitching. J Comp Sci Technol 1997;57:91–8.
[15] Pang F. A study of the creep behaviour of stitched woven composites, Ph.D. thesis, Deakin University, Australia, August 1998.